Systematics in SNS nEDM Experiment

Chris Swank, Bob Golub

Systematic Errors

- Geometric phase from magnetic gradients
  - Gradients natural to coil geometry
  - Magnetic impurities in cell walls, cell coatings, magnetic dust on coatings.
  - SQUID pick up leads distort d-c fields

Visualization: phase shifts from interaction of E and non-uniform B fields

Geometry

- Rectangular cell
- Assume $\omega_0 << 1/\tau_{wall}$
- Spin Starts on the Left wall.

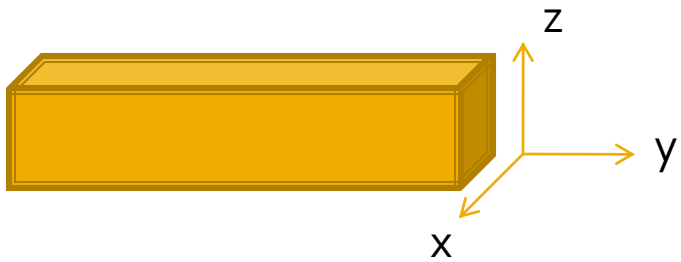

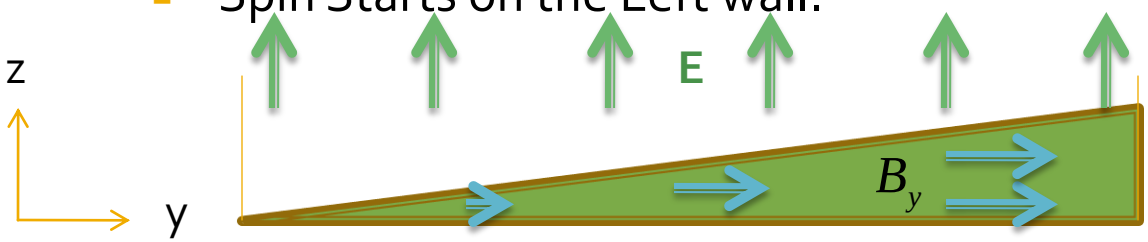

$B_y(0) < \langle B_y \rangle$

Slower Rotation about y

$B_y(L_y) > \langle B_y \rangle$

Faster Rotation about y

- y rotation from small field in y
- x rotation from v×E field.

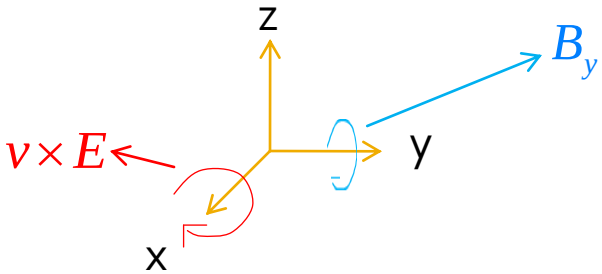

Visualization: phase shifts from E and non-uniform B fields

Spin Starts

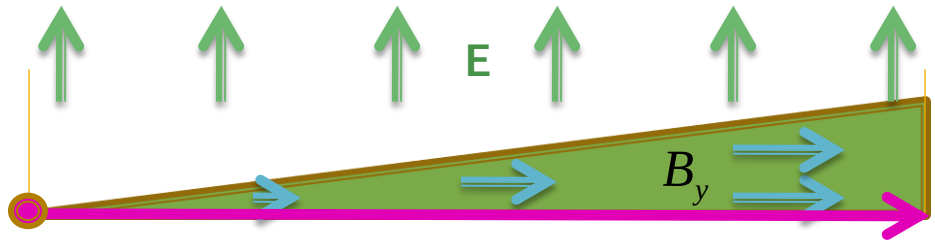

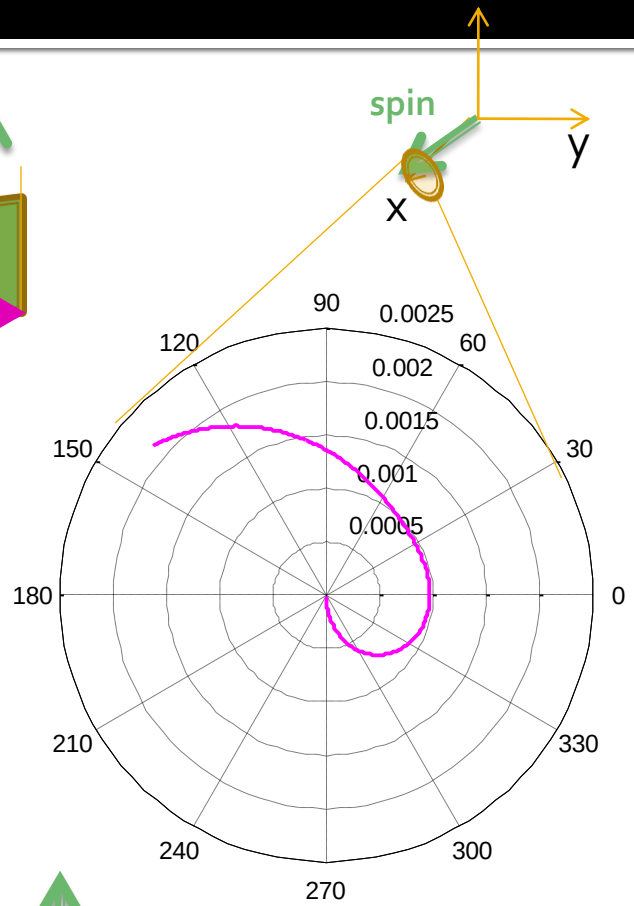

Phase after one length

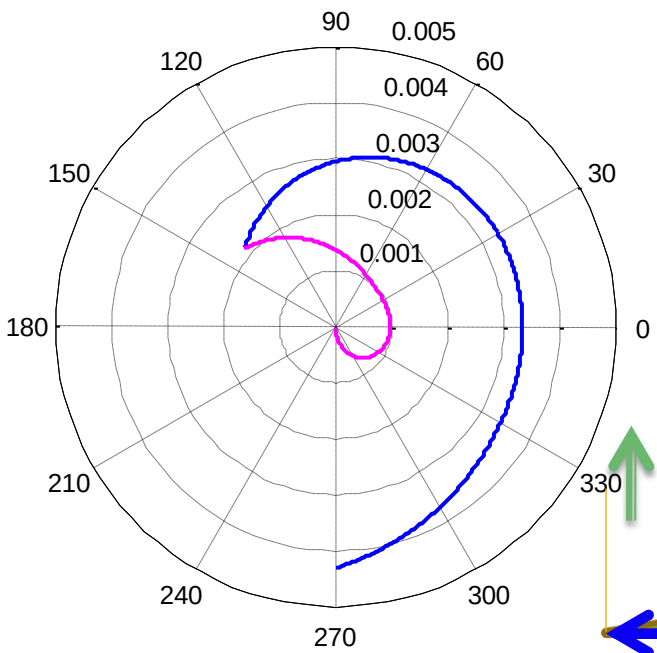

Phase after 1 round trip.

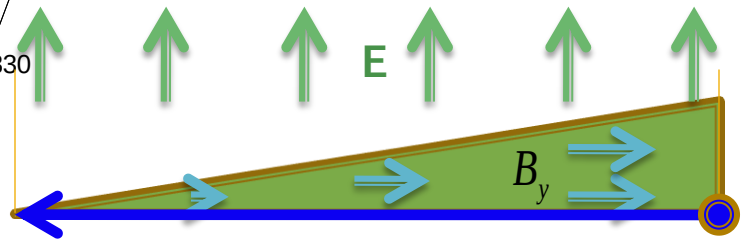

Spin Reflects and Travels Back

Correlation function theory to describe Geometric Frequency Shift (or any 2nd order effect)

- Derived from 2nd order density matrix formalism
- Spectrum of the field-position correlation function

$$\delta\omega = \omega_0 \frac{\gamma^2 E}{2c} \Im \left\{ \int_{-\infty}^{\infty} d\tau e^{-i\omega_0 \tau} \left\langle B_x(t)x(t+\tau) + B_y(t)y(t+\tau) \right\rangle \right\} - \frac{\gamma^2 E}{c} \left\langle B_x x + B_y y \right\rangle$$

field-position correlation function

field-position volume average

S. K. Lamoreaux and R. Golub. Detailed discussion of a linear electric field frequency shift induced in confined gases by a magnetic field gradient: Implications for neutron electric-dipole-moment experiments. *Physical Review A*, 71(3):032104(10), 2005.

Steven M. Clayton. Spin relaxation and linear-in-electric-field frequency shift in an arbitrary, time-independent magnetic field. *Journal of Magnetic Resonance*, 211(1):89–95, 2011.

Guillaume Pignol, Stephanie Roccia. Electric-dipole-moment-searches: Reexamination of frequency shifts for particles in traps. *Physical Review A*, 84(4):042105(5), 2012.

Swank. C.M., PhD thesis, North Carolina State University, Raleigh, NC, 2012

Correlation functions Beyond Diffusion Theory

- When $\lambda \sim L$ the diffusion equation does not accurately describe the correlation function

- Accurate description of correlation function necessary.
  - Simulation of the continuous time random walk

  OR

  - Exact solution of the continuous time random walk.

The Correlation Function in 1-D

Solution to the telegraphers equations satisfies isotropic Boltzmann transport in 1D

$$p(x,t|x_0,0) = \frac{1}{L}\sum_{n=-\infty}^{\infty} e^{-\frac{t}{2\tau_c}}\left\{\cos\left(\frac{n\pi x_0}{L} - \frac{is_n t}{2\tau_c}\right) + \frac{i}{s_n}\sin\left(\frac{n\pi x_0}{L} - \frac{is_n t}{2\tau_c}\right)\right\}$$

$$s_n = \sqrt{1 - 4\omega_n^2\tau_c^2}, \quad \omega_n = \frac{n\pi v}{L}$$

$$\langle H_x(t)x(t+\tau)\rangle = \int_0^L dx_0 G_x x_0 p(x_0,t)\int_0^L x p(x,t+\tau|x_0,t)dx$$

$$H_{xx}(\omega) = \frac{2G_x v^2\tau_c^3}{\pi^2}\sum_{n=-\infty}^{\infty}\frac{1}{\left(\frac{1}{2}+n\right)^2\left((\omega^2-\omega_n^2)^2\tau_c^4 + \frac{\omega^2}{\tau_c^2}\right)}$$

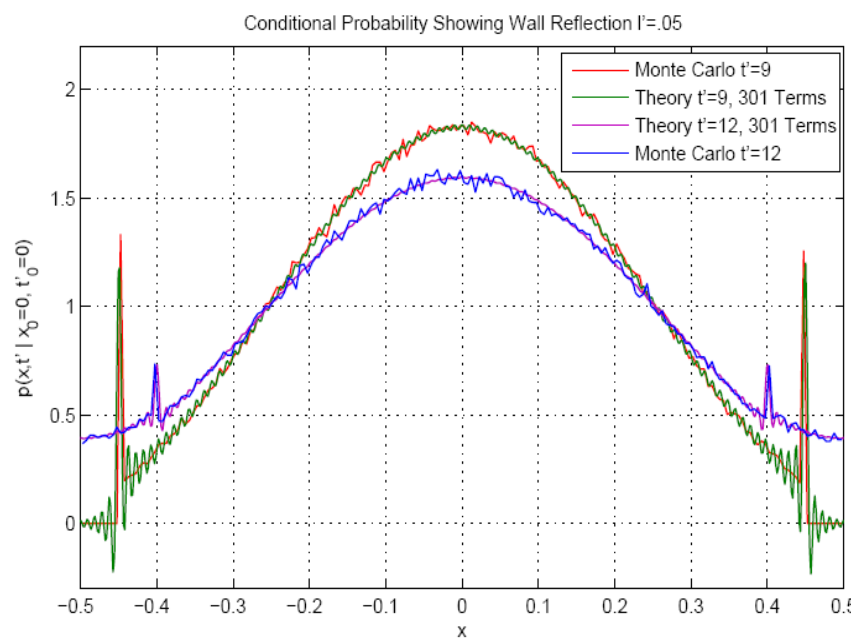

Valid for Diffusion
Valid for Ballistic motion

[1] C. Swank and R. Golub. arXiv:1012.4006 2010.

2D & 3D Conditional densities.

Spectrum for the infinite region continuous time random walk in 2D

2D
$$p(Q,s) = \frac{1}{\sqrt{(\frac{1}{\tau_c}+s)^2 + v^2Q^2} - \frac{1}{\tau_c}}$$

The infinite region 3D spectrum

3D
$$p(Q,s) = \frac{\arctan\left(\frac{vQ}{\frac{1}{\tau_c}+s}\right)}{vQ - \frac{1}{\tau_c}\arctan\left(\frac{vQ}{\frac{1}{\tau_c}+s}\right)}$$

Masoliver, J., Porrá, J.M. and Weiss, G.H., Phys Rev **E48**, 939 (1993)

Restricted random walk

2D Trajectory Visualization

Shown are a few trajectories that are seen by an observer

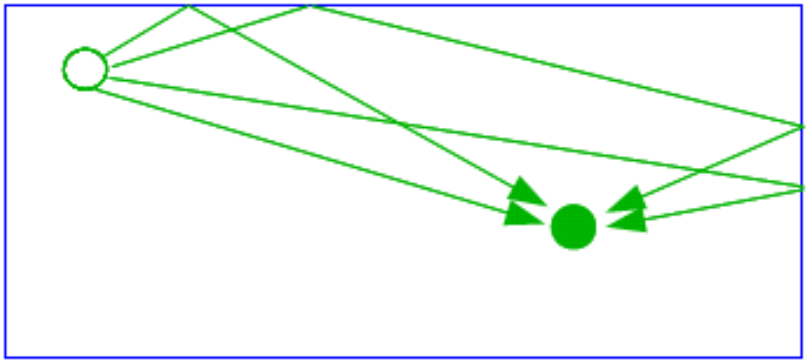

Source Observer

Restricted random walk

2D Trajectory Visualization
The picture reversed.

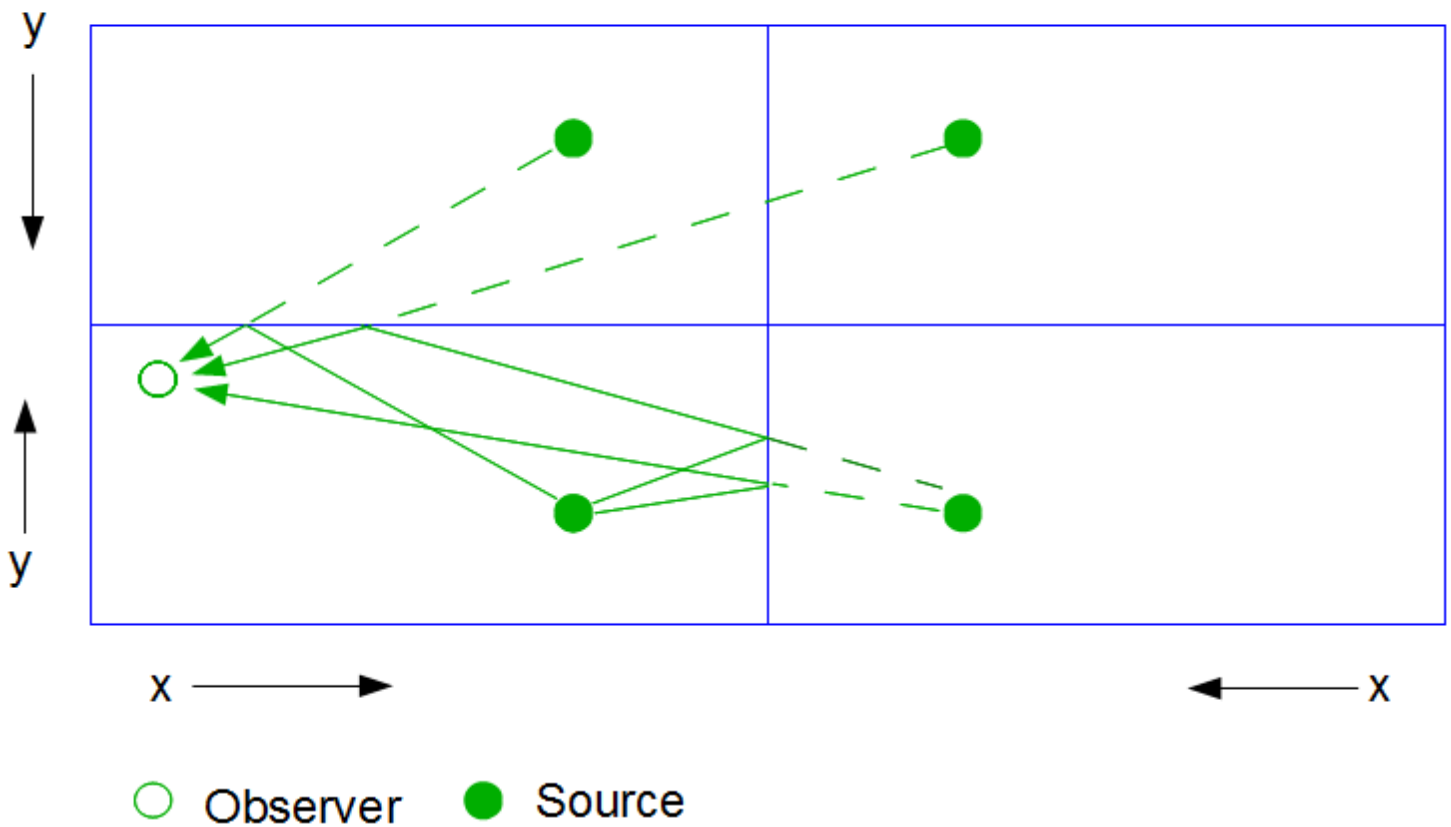

Restricted random walk

(Specular wall scattering required for dimensions > 1)

2D Trajectory Visualization
Image cells

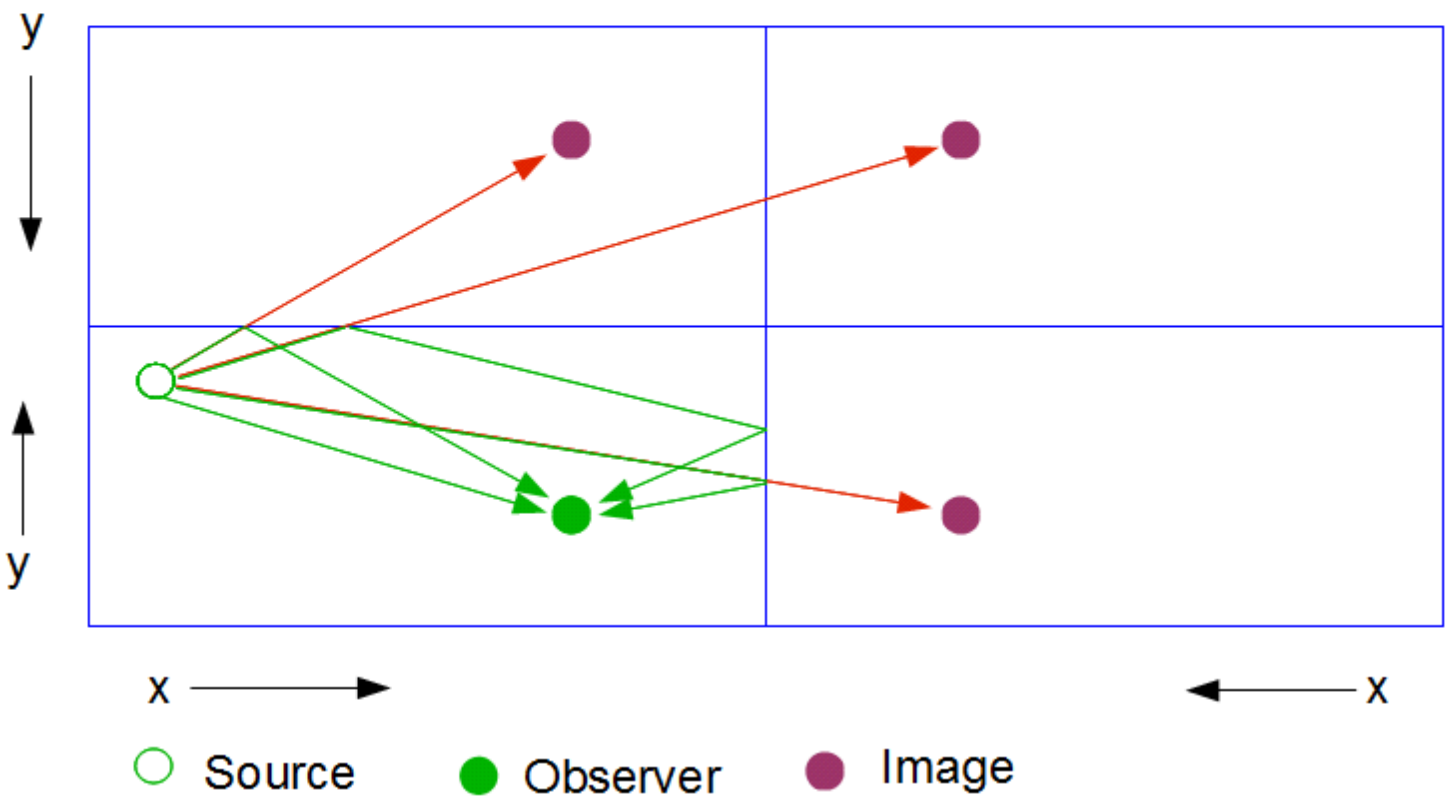

Field reversed with cell images

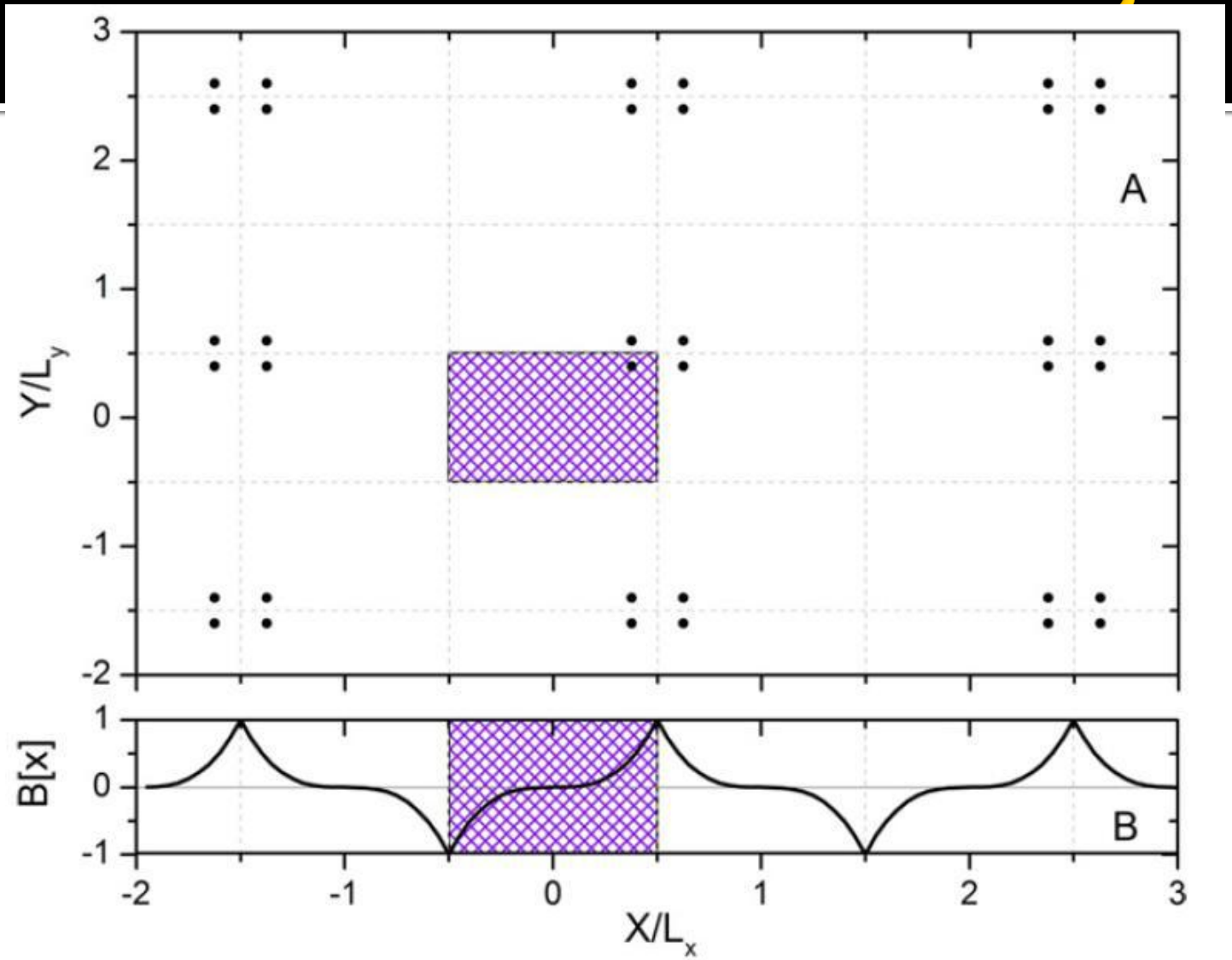

C.M. Swank, A.K. Petukhov and R. Golub. Correlation functions for restricted brownian motion from the ballistic through to the diffusive regimes. *Physics Letters A*, 376(34):2319–2324, 2012.

Restricted random walk

Therefore the solution to the restricted conditional probability is defined from

$$
\begin{aligned}
r &= \sqrt{(x-x_0)^2+(y-y_0)^2} \\
x_l, y_l &= 2l_{x,y}L_{x,y} \pm x, y \\
p_{rect}(x,y,t) &= \sum_{l_{x,y}=-\infty}^{\infty} p(x_l, y_l, t)
\end{aligned}
$$

And 3D (will be used.)

$$
\begin{aligned}
r &= \sqrt{(x-x_0)^2+(y-y_0)^2+(z-z_0)^2} \\
x_l, y_l, z_l &= 2lL_{x,y,z} \pm x, y, z \\
p_{rect}(x,y,t) &= \sum_{l_{x,y,z}=-\infty}^{\infty} p(x_l, y_l, z_l, t)
\end{aligned}
$$

The geometric frequency shift derived from the restricted random walk

Define the spectrum.

$$S_B(\omega) = \int_{-\infty}^{\infty} \langle B(t)B(t+\tau)\rangle \, \mathrm{e}^{-i\omega\tau} d\tau$$

Written in terms of the 3D conditional probability.

$$S_B(\omega) = \frac{1}{(2\pi)^3} \int_V \mathbf{B}(\mathbf{x_0}) d^3\mathbf{x_0} \int_{-\infty}^{\infty} \widetilde{\mathbf{B}}(\mathbf{x}) d^3\mathbf{x} \int d\omega \int d^3\mathbf{Q} \mathrm{e}^{i\mathbf{Q}\cdot(\mathbf{x_0}-\mathbf{x})+i\omega\tau} \boxed{p(\mathbf{Q},\omega)}$$

One can take advantage of the periodicity of the variables via Fourier series, Simplifying the integration.

$$\int_{-\infty}^{\infty} \widetilde{\mathbf{B}}(\mathbf{x}) d^3\mathbf{x} \mathrm{e}^{-i\mathbf{Q}\cdot\mathbf{x}} = (2\pi)^3 \sum_{l_x,l_y,l_z=-\infty}^{\infty} \int_{-\frac{L_x}{2}}^{\frac{3L_x}{2}} \int_{-\frac{L_y}{2}}^{\frac{3L_y}{2}} \int_{-\frac{L_z}{2}}^{\frac{3L_z}{2}} d^3\mathbf{x}\mathbf{B}(\mathbf{x}) \ldots$$

$$\times \mathrm{e}^{-i\mathbf{Q}\cdot\mathbf{x}} \delta(Q_x - \frac{l_x\pi}{L_x}) \delta(Q_y - \frac{l_y\pi}{L_y}) \delta(Q_z - \frac{l_z\pi}{L_z})$$

The geometric frequency shift derived from the restricted random walk

The integration is a sum over the Fourier components of the field.

$$S_B(\omega) = \sum_{l_x,l_y,l_z=-\infty}^{\infty} B_0(l_x,l_y,l_z)B(l_x,l_y,l_z)p\left(\left[\frac{l_x\pi}{L_x},\frac{l_y\pi}{L_y},\frac{l_z\pi}{L_z}\right],\omega\right)$$

$$B_0(l_x,l_y,l_z) = \sum_{l_x,l_y,l_z=-\infty}^{\infty} \int_{-\frac{L_x}{2}}^{\frac{L_x}{2}}\int_{-\frac{L_y}{2}}^{\frac{L_y}{2}}\int_{-\frac{L_z}{2}}^{\frac{L_z}{2}} \mathbf{B}(\mathbf{x}_0)\mathrm{e}^{i\pi\left(\frac{l_x x_0}{L_x}+\frac{l_y y_0}{L_y}+\frac{l_z z_0}{L_z}\right)}d^3\mathbf{x}_0$$

$$B(l_x,l_y,l_z) = \sum_{l_x,l_y,l_z=-\infty}^{\infty} \int_{-\frac{L_x}{2}}^{\frac{3L_x}{2}}\int_{-\frac{L_y}{2}}^{\frac{3L_y}{2}}\int_{-\frac{L_z}{2}}^{\frac{3L_z}{2}} \mathbf{B}(\mathbf{x})\mathrm{e}^{-i\pi\left(\frac{l_x x}{L_x}+\frac{l_y y}{L_y}+\frac{l_z z}{L_z}\right)}d^3\mathbf{x}$$

The position autocorrelation function spectrum in different dimensions

$$S_{1D}(\omega) = \sum_{n=\text{integers}} \frac{2v\tau_c}{\left(\frac{1}{2}\pi+n\pi\right)\left(\left(\omega^2-\omega_n^2\right)^2\tau_c^4+\tau_c\omega^2\right)},$$

$$\omega_n = \frac{\pi\left(2n+1\right)}{L_x}, \quad n = \text{integers}$$

$$S_{2D}(\omega) = \sum_{lx=odd} \frac{8L_x^2}{\pi^4 l_x^4}\frac{1}{\sqrt{\left(\frac{1}{\tau_c}+i\omega\right)^2+\frac{v^2\pi^2 l_x^2}{L_x^2}}-\frac{1}{\tau_c}},$$

$$l_x = \text{odd integers.}$$

$$S_{3D}(\omega) = \sum_{lx=odd} \frac{8L_x^2\tau_c}{\pi^4 l_x^4}\frac{1}{\frac{q_x}{\arctan\left(\frac{q_x}{1+i\omega\tau_c}\right)}-1}$$

$$q_x = \frac{\pi l_x v\tau_c}{L_x}, \quad lx = \text{odd integers.}$$

Comparison of Different Dimensions

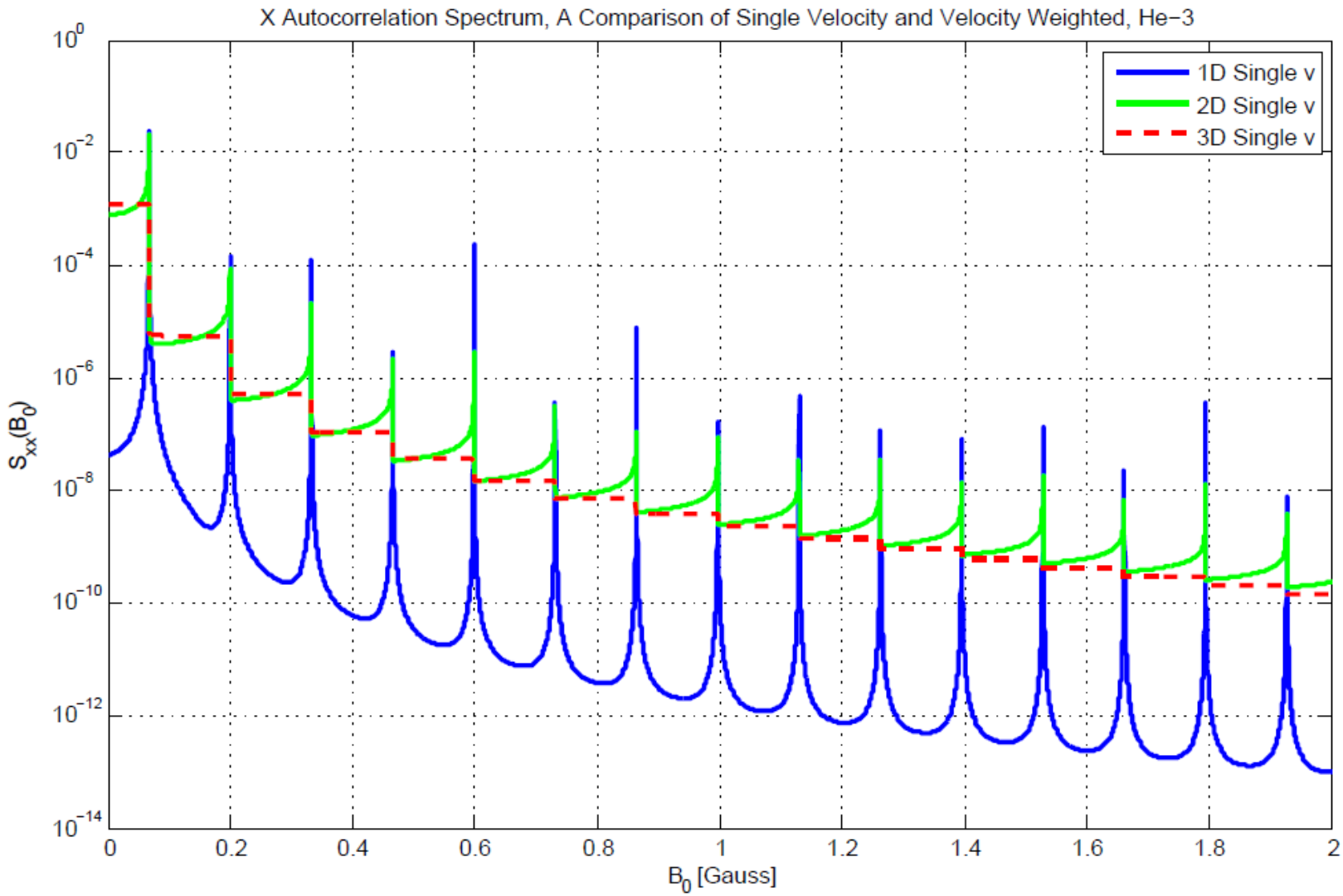

Velocity Weighted Distributions

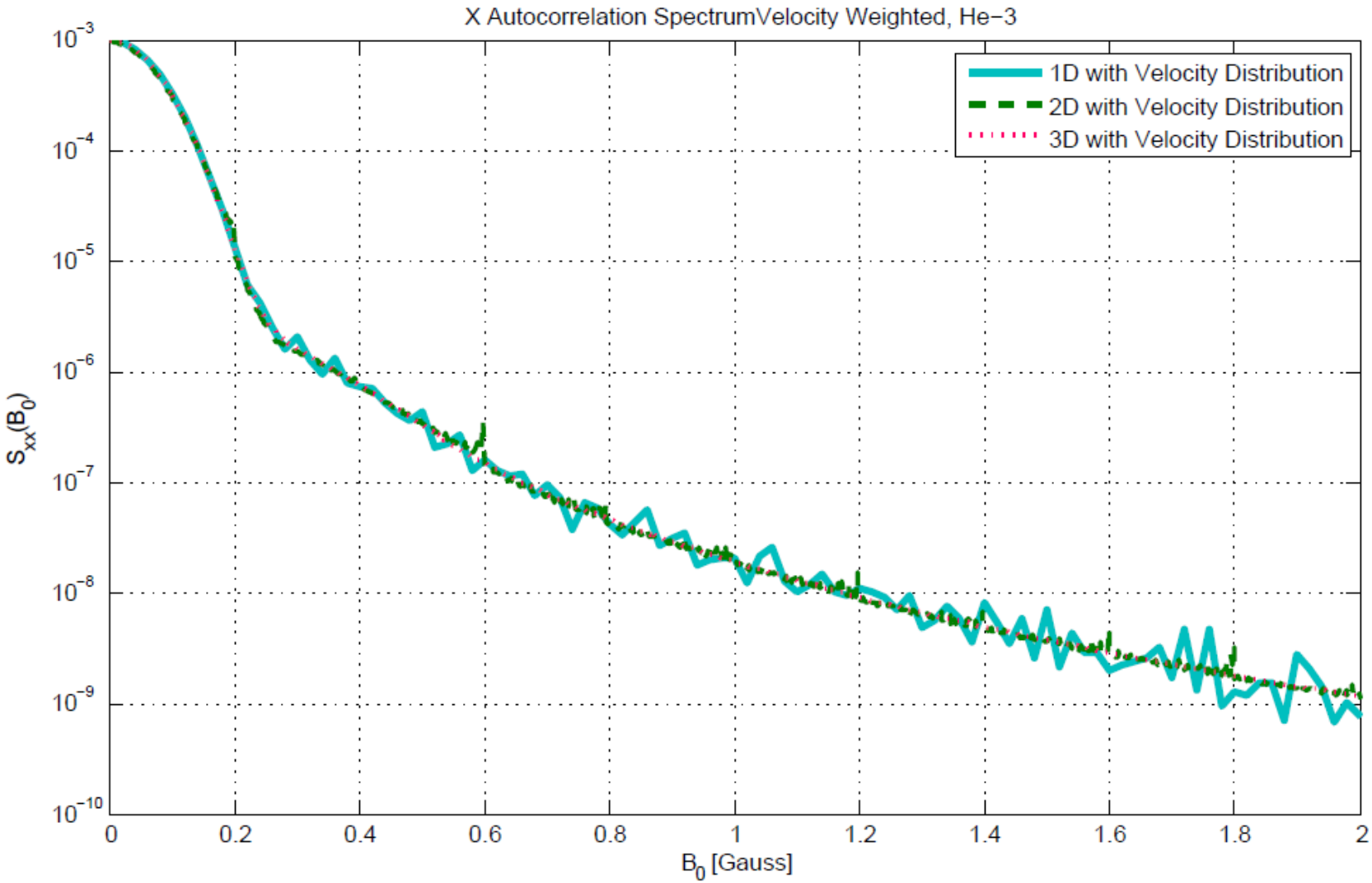

False EDM due to frequency shift

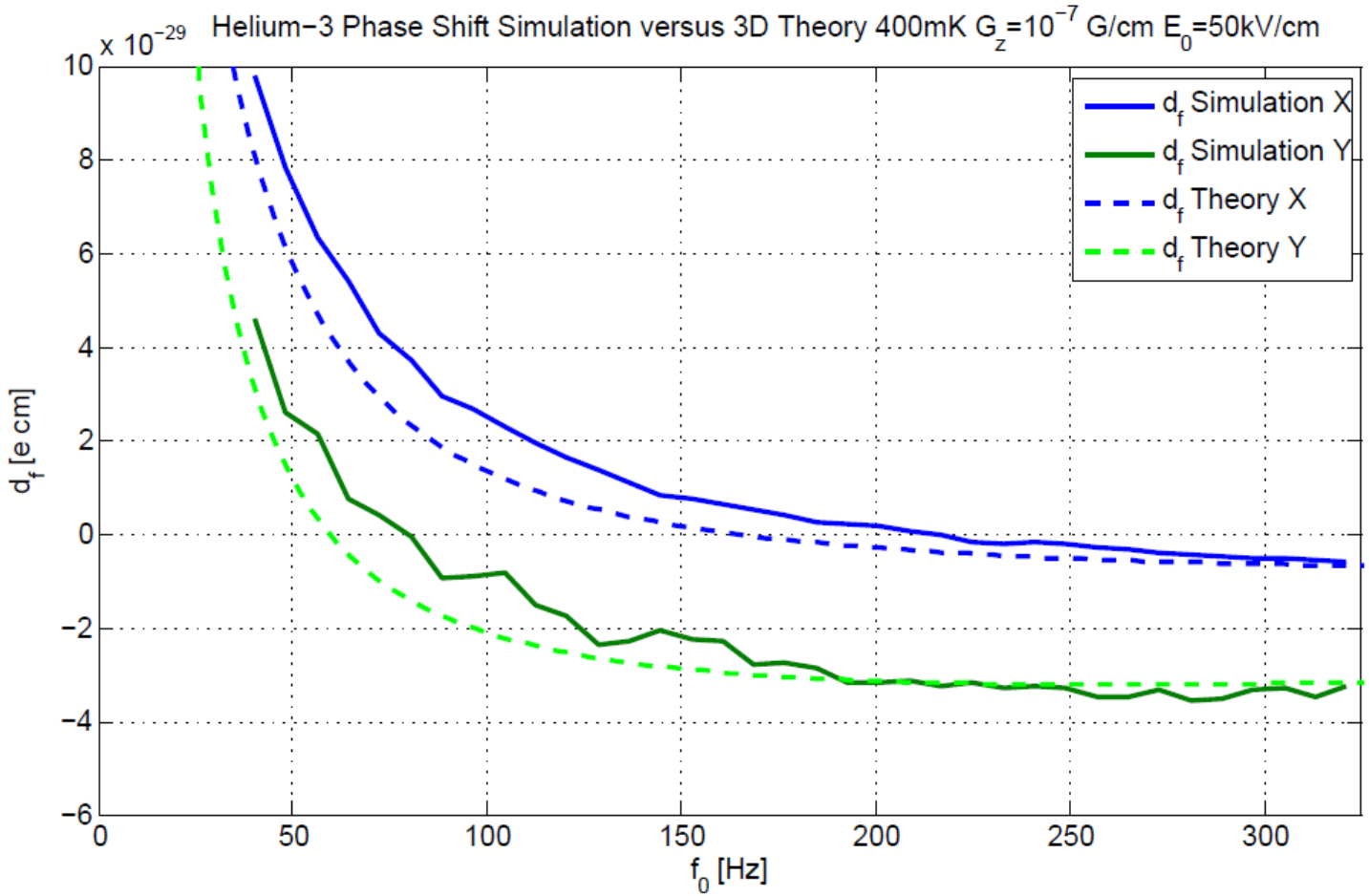

$$\Delta\omega = \frac{2ed_n\Delta E}{\hbar}$$

$$d_f = 4.56 \times 10^{-29} S(\omega)$$

X=10.2 cm
Y=40 cm

Figure 2.9: Comparison of the simulated false EDM in helium-3 versus the 3D theory 400mK. 200,000 particles where simulated.

Gradient Relaxation Measurements

$$\frac{1}{T_{1gradient}} = \frac{\gamma^2 \left(\frac{G_z}{2}\right)^2}{2} \left(S_{xx}(\omega_0) + S_{yy}(\omega_0)\right)$$

FID Measured Relaxation is Given by:

$$\frac{1}{T_1} = \frac{1}{T_{1\,\mathrm{gradient}}} + \frac{1}{T_{1\,\mathrm{pulse}}} + \frac{1}{T_{1\,\mathrm{wall}}} + \frac{1}{T_{1\,\mathrm{spin}}}$$

Where the Pulse loss is calculated from

$$\frac{1}{T_{1\,\mathrm{pulse}}} = -\frac{\ln\left(\cos\left(\frac{\tau(\alpha)}{\tau\left(\frac{\pi}{2}\right)}\frac{\pi}{2}\right)\right)}{\Delta t}$$

The error propagates like

$$\left(\frac{\sigma_{T_{1Gradient}}}{T_{1Gradient}}\right)^2 = \left(\frac{\sigma_{T_{1Total}}}{T_{1Total}}\right)^2 + \left(\frac{\sigma_{Pulse}}{T_{1Pulse}}\right)^2 + \left(\frac{\sigma_{T_{1Wall}}}{T_{1Wall}}\right)^2$$

Low Temperature Apparatus

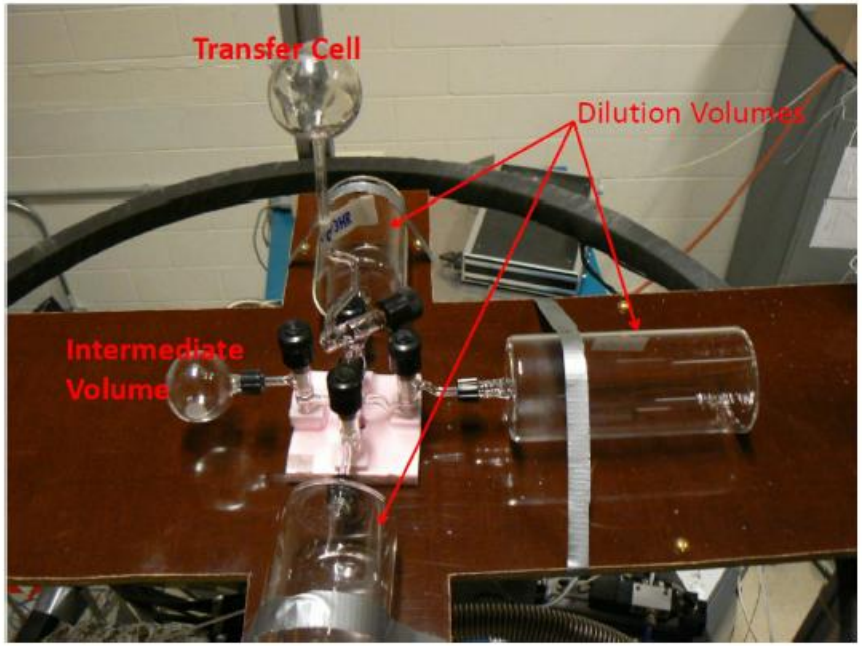

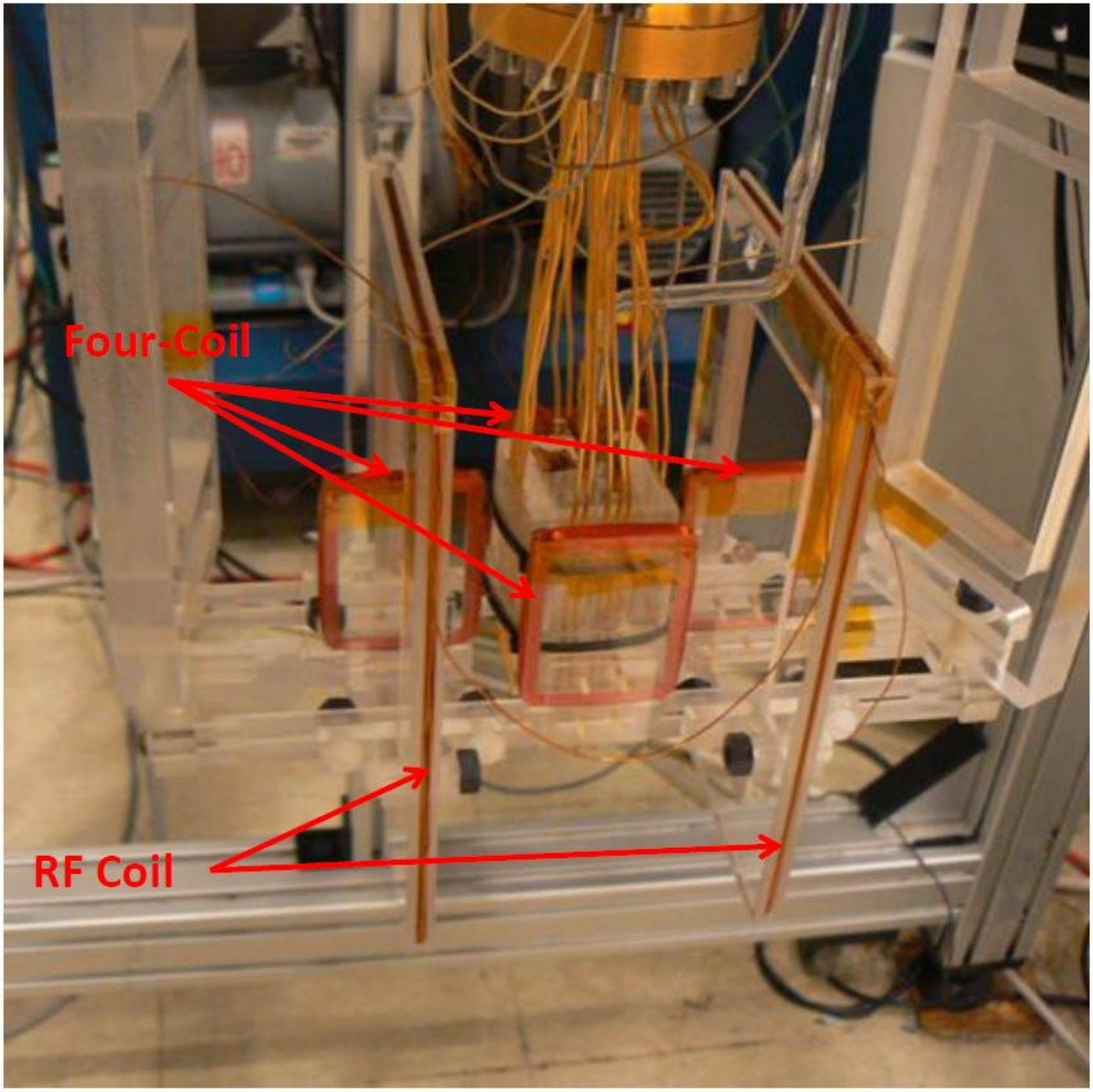
Four-Coil
RF Coil

Theory Predictions

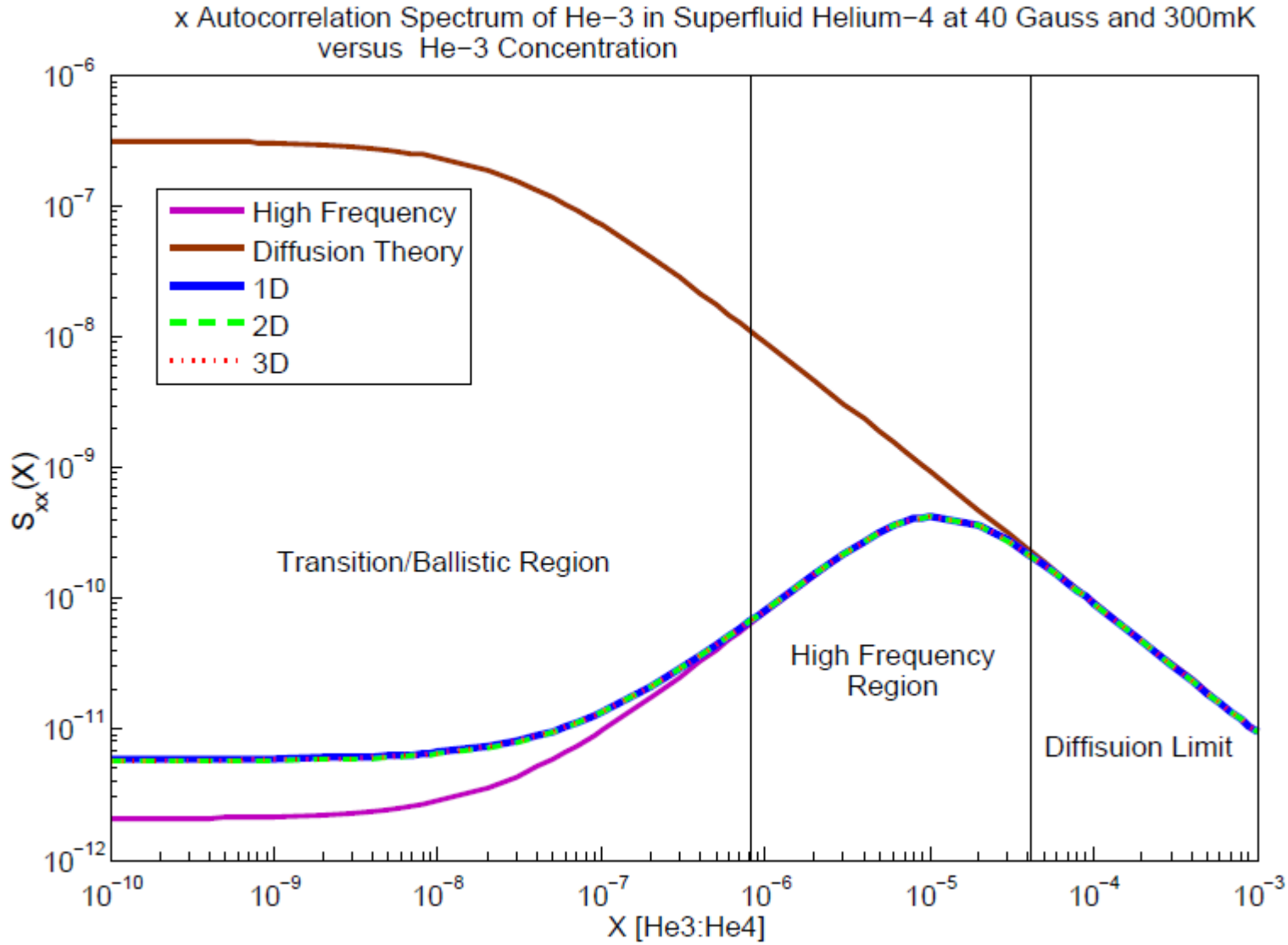

Data at 430 mK

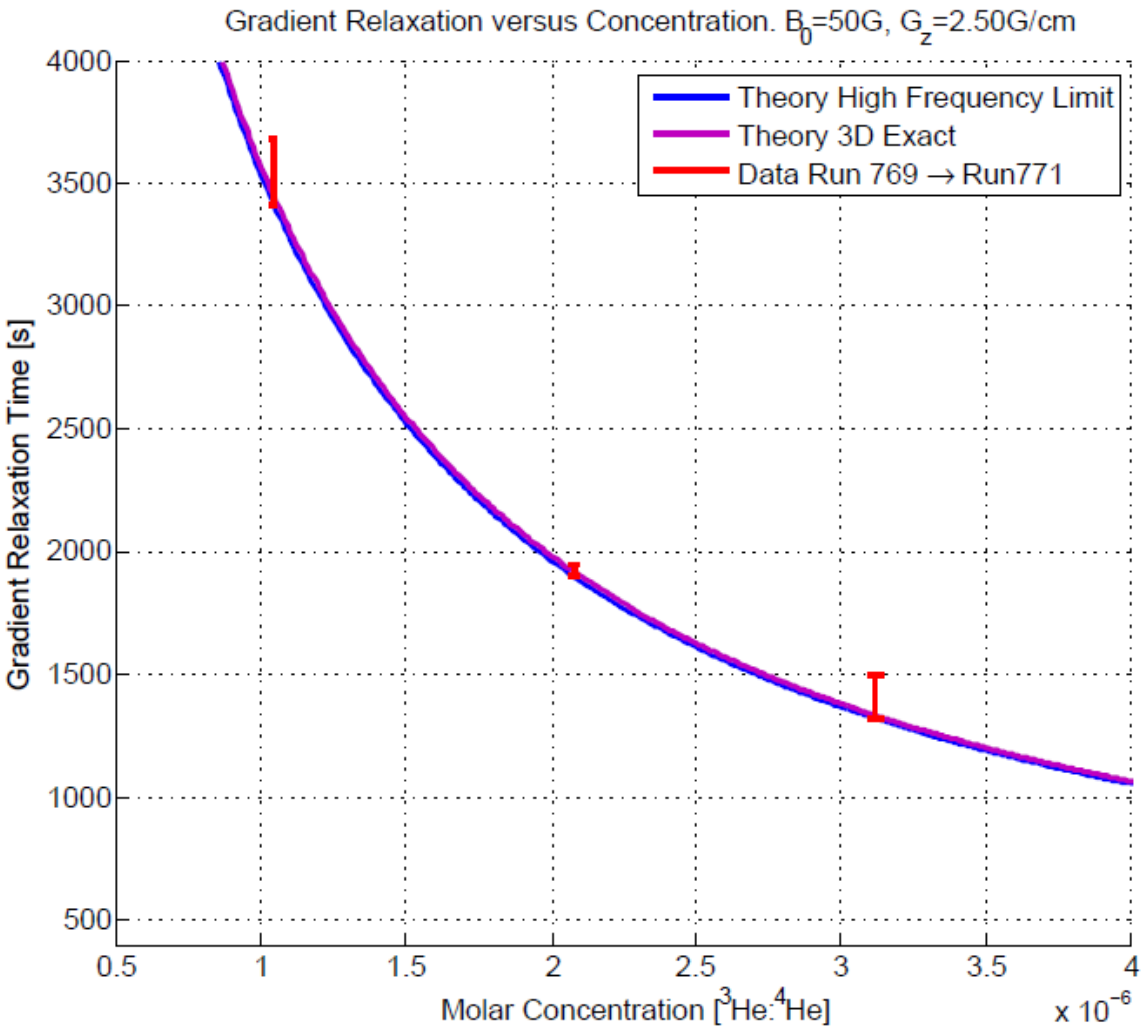

Neutron Frequency Shift

- Assume v^2 distribution
  - 165 neV maximum energy
- Completely ballistic motion

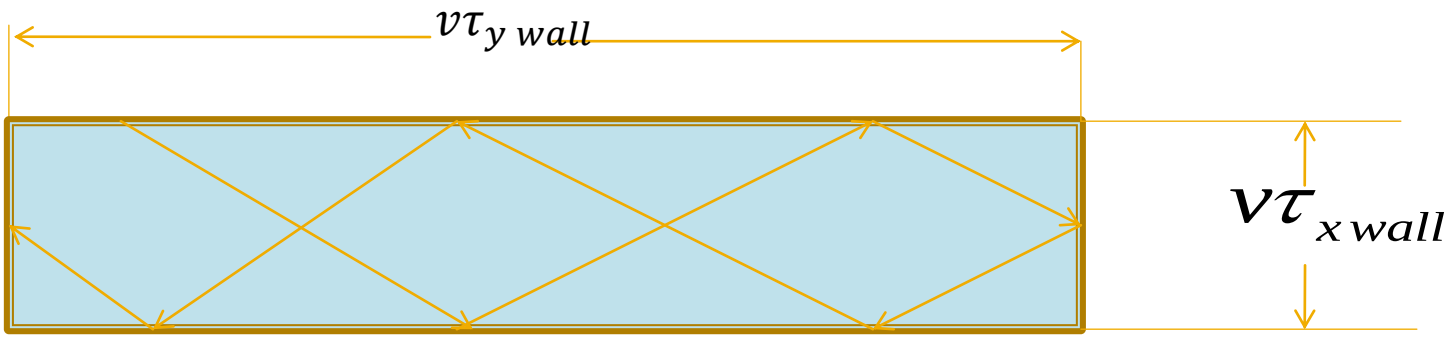

- Specular wall reflections?

Coatings under UV Lamp

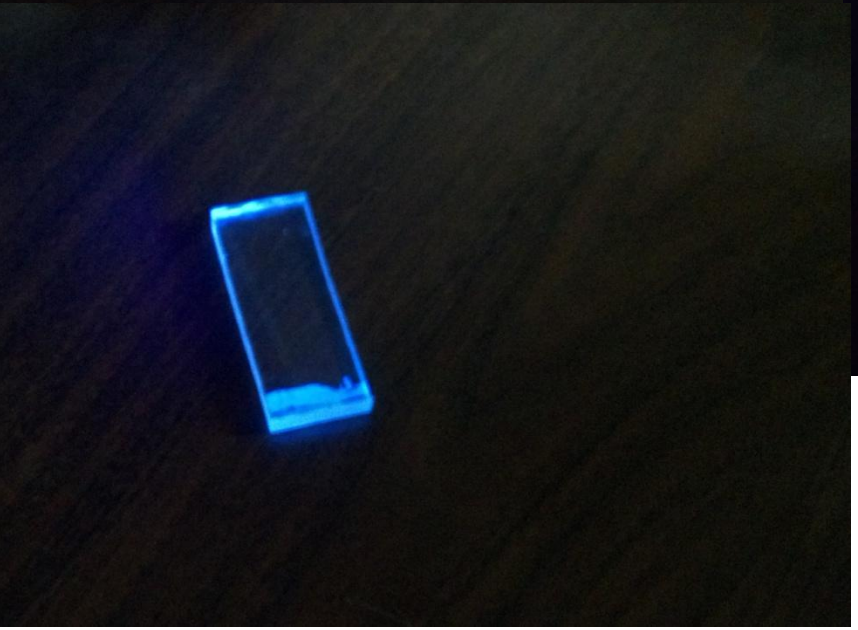

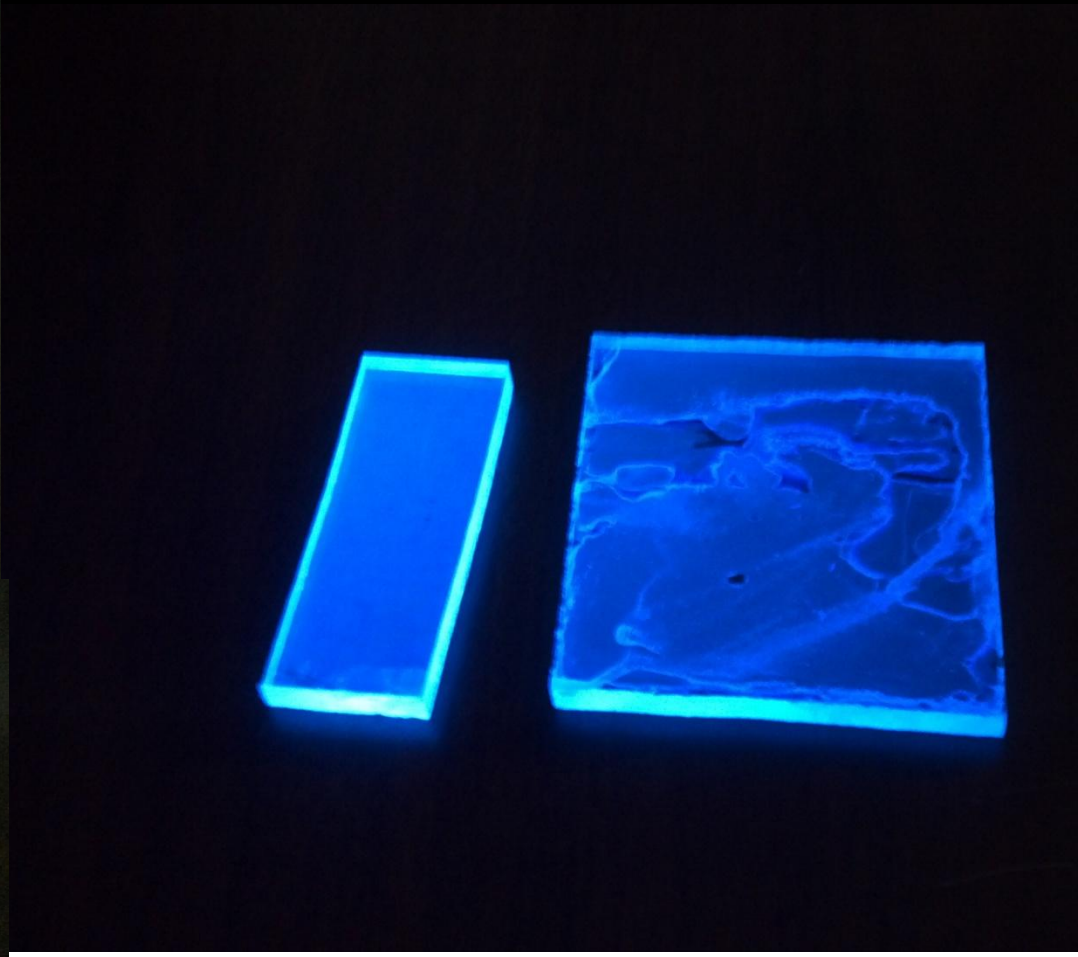

AFM Image

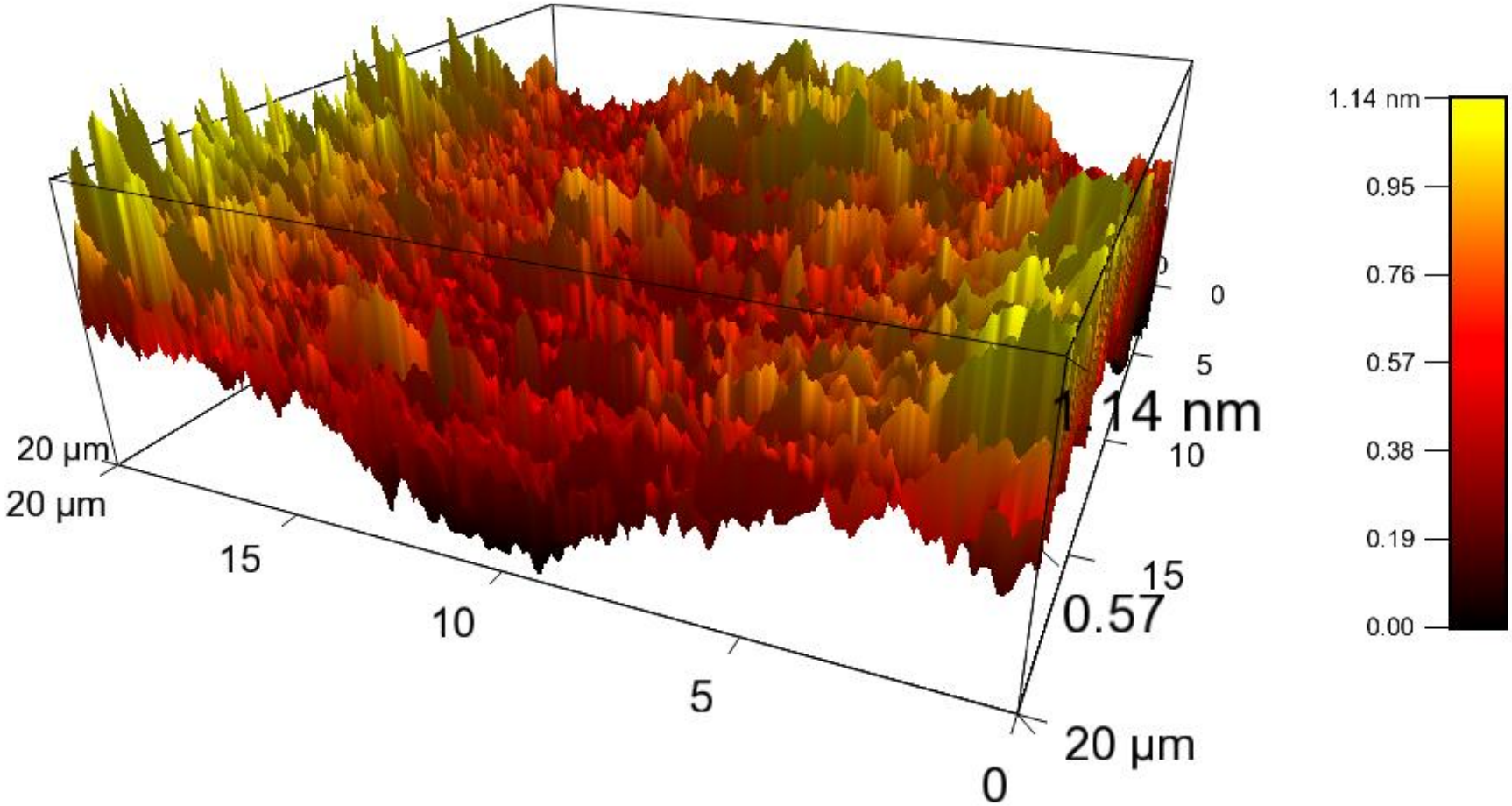
1.14 nm
0.95
0.76
0.57
0.38
0.19
0.00
20 µm
20 µm
15
10
5
0
0
5
10
15
20 µm
1.14 nm
0.57

AFM Images
Shows roughness on the ~1nm scale

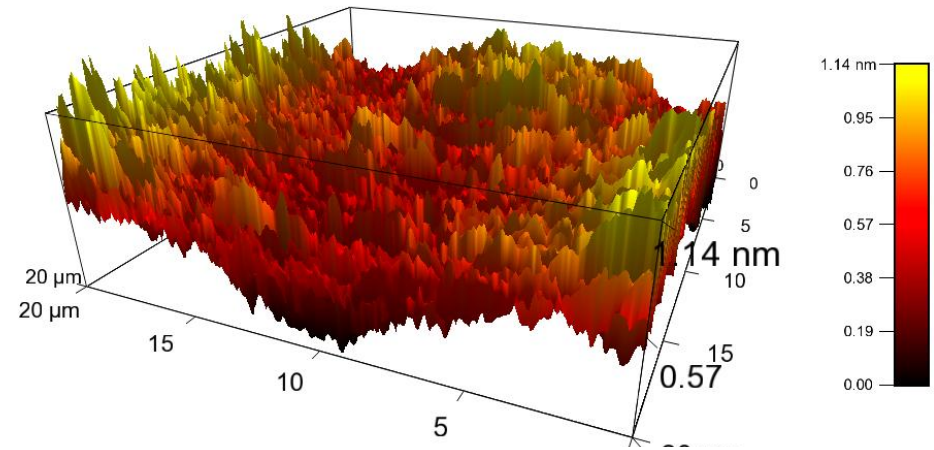

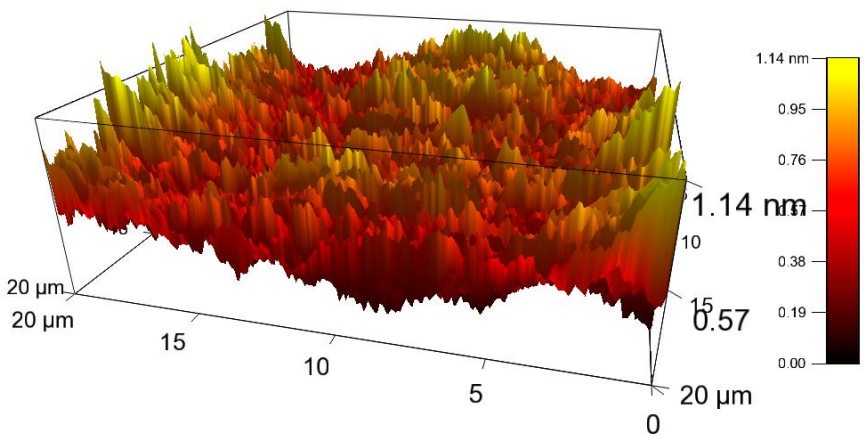

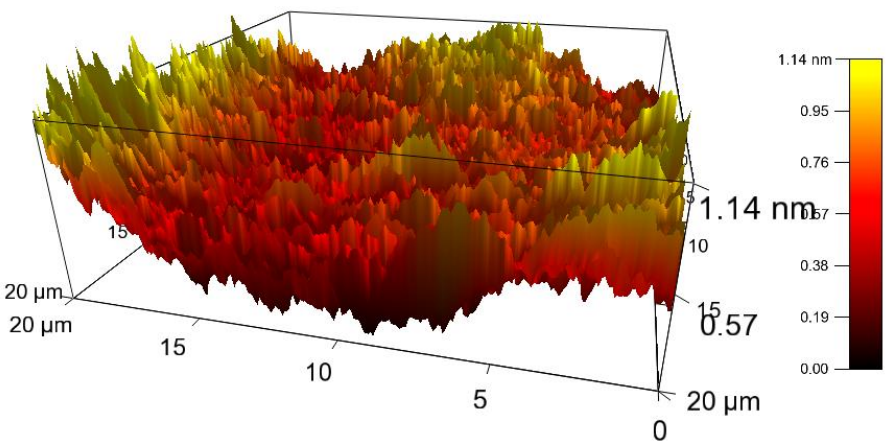

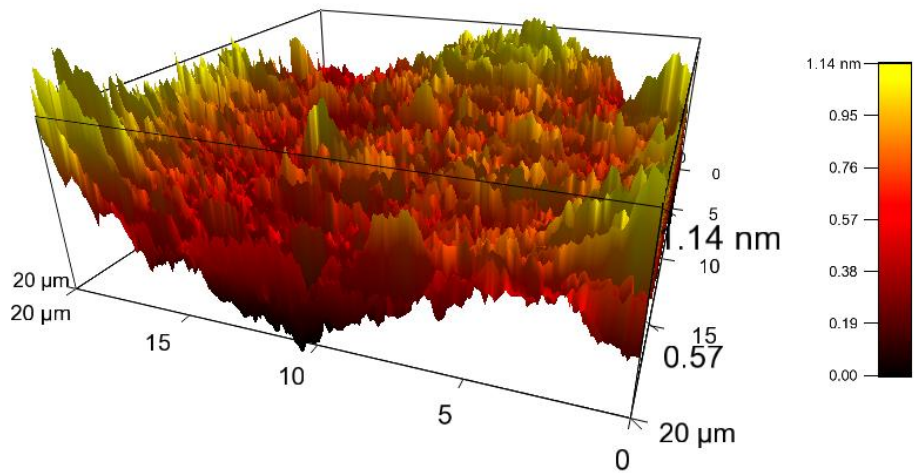

Wall collisions

From AFM setting

$b = 1\ nm$

$w = .1\ \mu m$

$$P_{ns}(\cos\theta_i) \equiv \int I_{ns}(\theta_2, \phi_2)\, d\Omega_2,$$

$$I_{ns}(\theta_2, \phi_2) = \frac{3}{2\pi}\frac{4\ k^4 w^2 b^2}{3}\cos\theta_i \cos^2\theta_2 \exp -\frac{w^2 k^2}{2} \times \left(\sin^2\theta_i + \sin^2\theta_2 - 2\sin\theta_i \sin\theta_2 \cos\phi_2\right)$$

$P(\perp) \sim 1\%$

[A Steyerl, Z Physic, 254, 1972]
[V. K. Ignatovich, JINR, p4-7055, 1973]
[M. Brown, R. Golub, J. M. Pendelbury. Vacuum Vol. 25 num 2, 1974]

Neutron Phase shift from Theory.

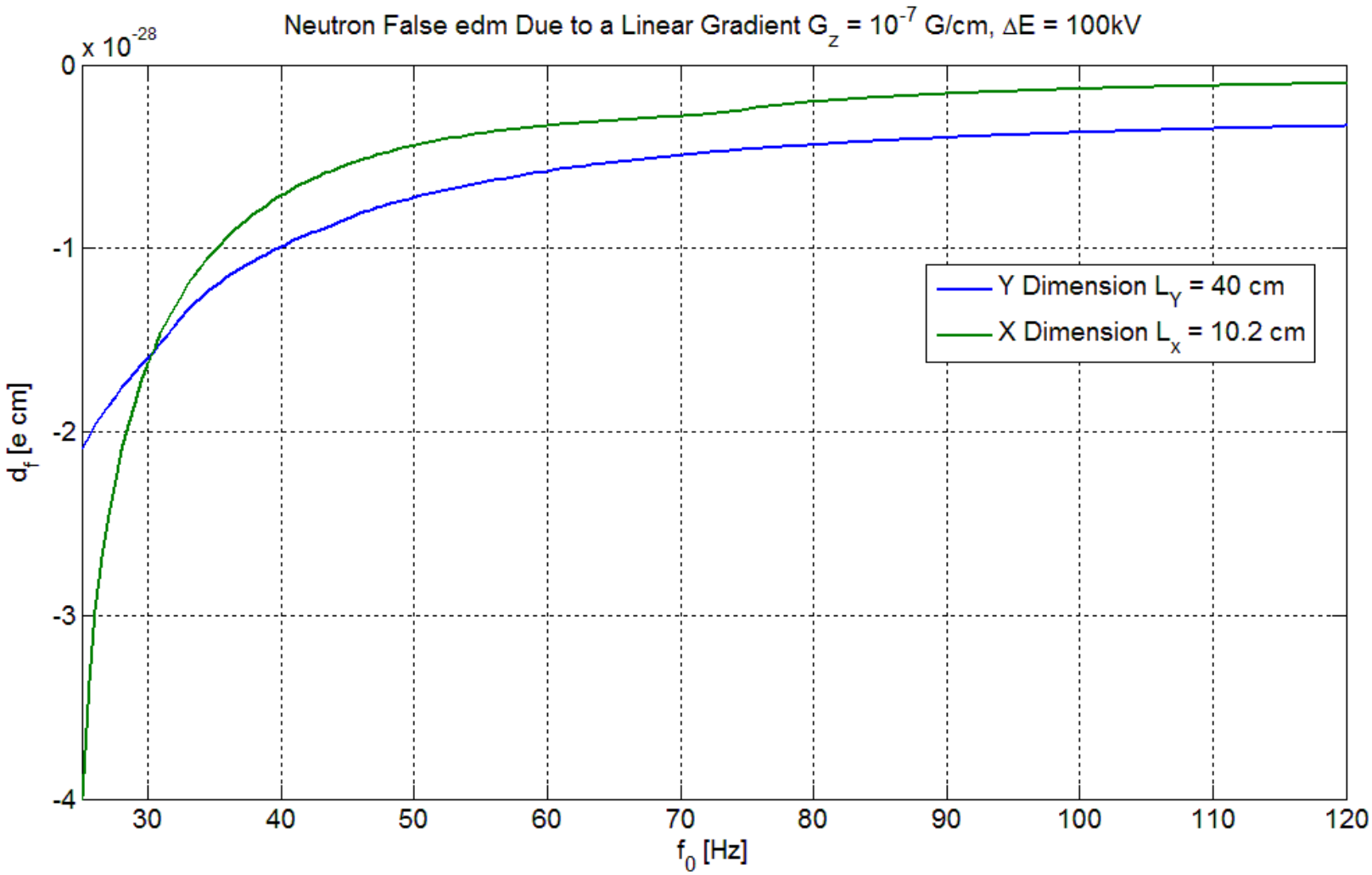

Magnetic impurities

- For (small) magnetic impurities the correlation time is small

$$\delta\omega = \omega_0 \frac{\gamma^2 E}{2c} \Im \left\{ \int_{-\infty}^{\infty} d\tau e^{-i\omega_0 \tau} \left\langle B_x(t) x(t+\tau) + B_y(t) y(t+\tau) \right\rangle \right\} - \frac{\gamma^2 E}{c} \left\langle B_x x + B_y y \right\rangle$$

≈ 0

$$\delta\omega = -\frac{\gamma^2 E}{c} \langle B_x x + B_y y \rangle$$

Guillaume Pignol, Stephanie Roccia. Electric-dipole-moment-searches: Reexamination of frequency shifts for particles in traps. *Physical Review A*, 84(4):042105(5), 2012.

Shift from contaminant.

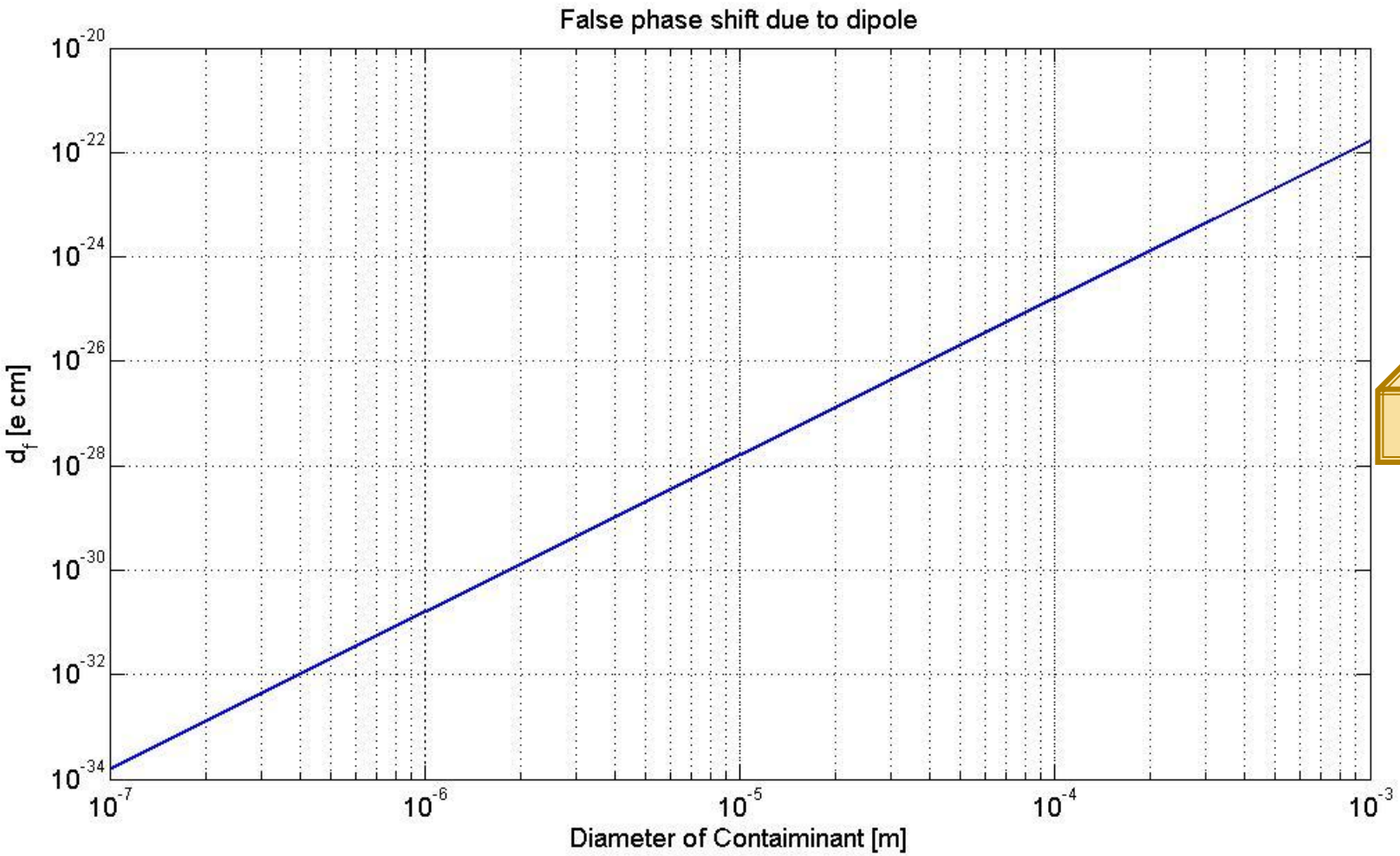

M= $0.2\ T$

Dipole Detection

- Cs NMOR magnetometer for testing.

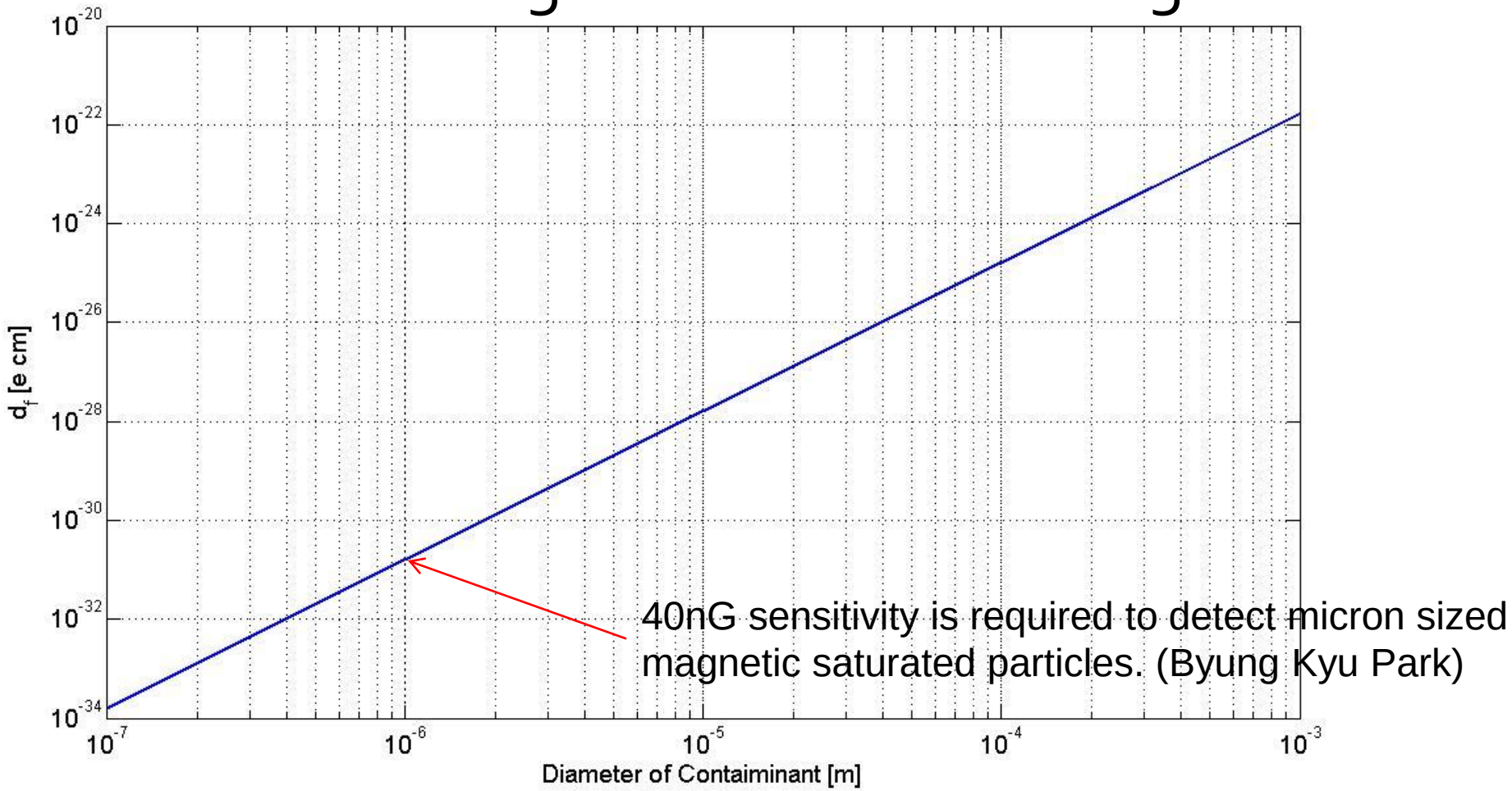

https://nedm.bu.edu/twiki/pub/NEDM/Collab021011Agenda/dipole_detection.pdf

Field Distortion from SQUID Pickup coils

- 3mm OD round wire

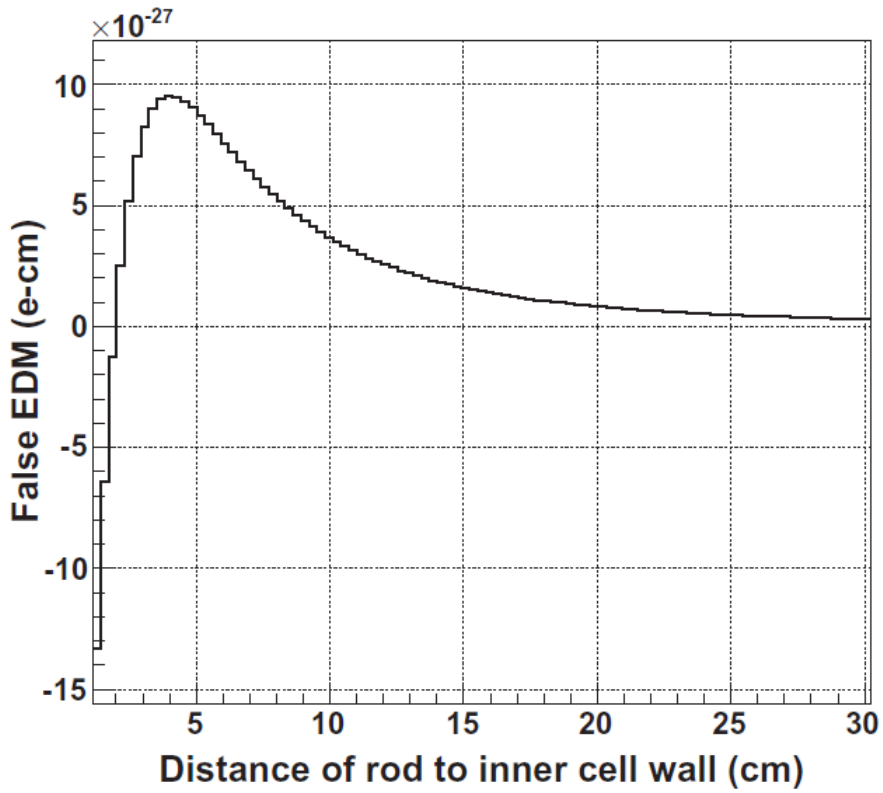

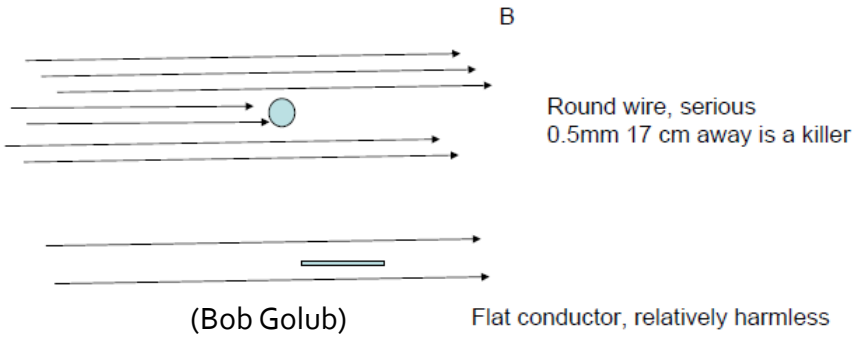

Steven M. Clayton. Spin relaxation and linear-in-electric-field frequency shift in an arbitrary, time-independent magnetic field. *Journal of Magnetic Resonance*, 211(1):89–95, 2011.

Actual SQUID flat loops

Thin film deposition

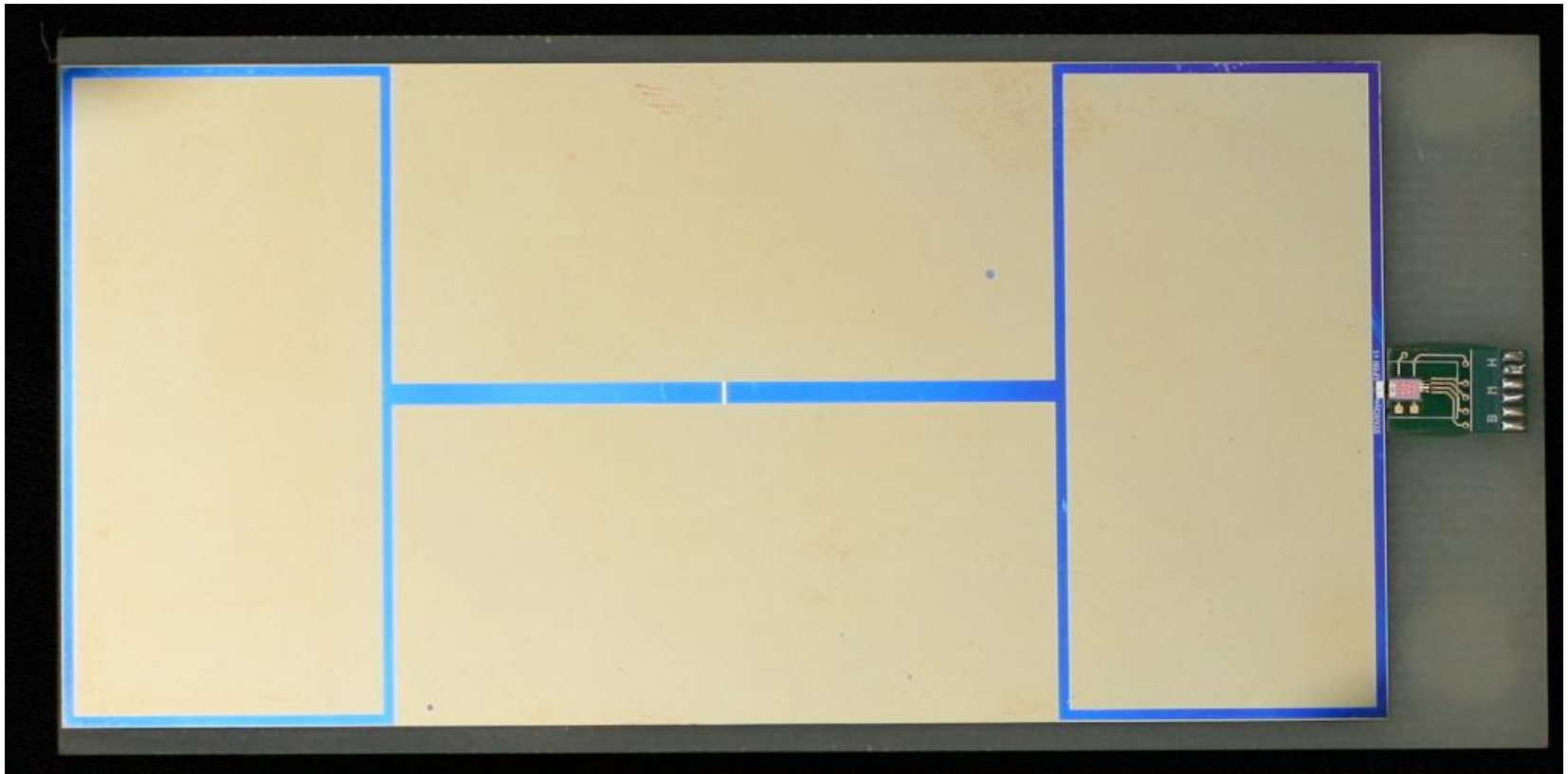

PULSTAR Systematic Studies

- Deuterium Source at NCSU PULSTAR reactor
- Correlation function studies via helium scintillation from $^{3}\mathrm{He}(\mathrm{n},\mathrm{p})^{3}\mathrm{H}$ with a Q-value of 764
- Critical Dressing Studies.
- Effects of magnetic impurities/gradients

PULSTAR Systematics

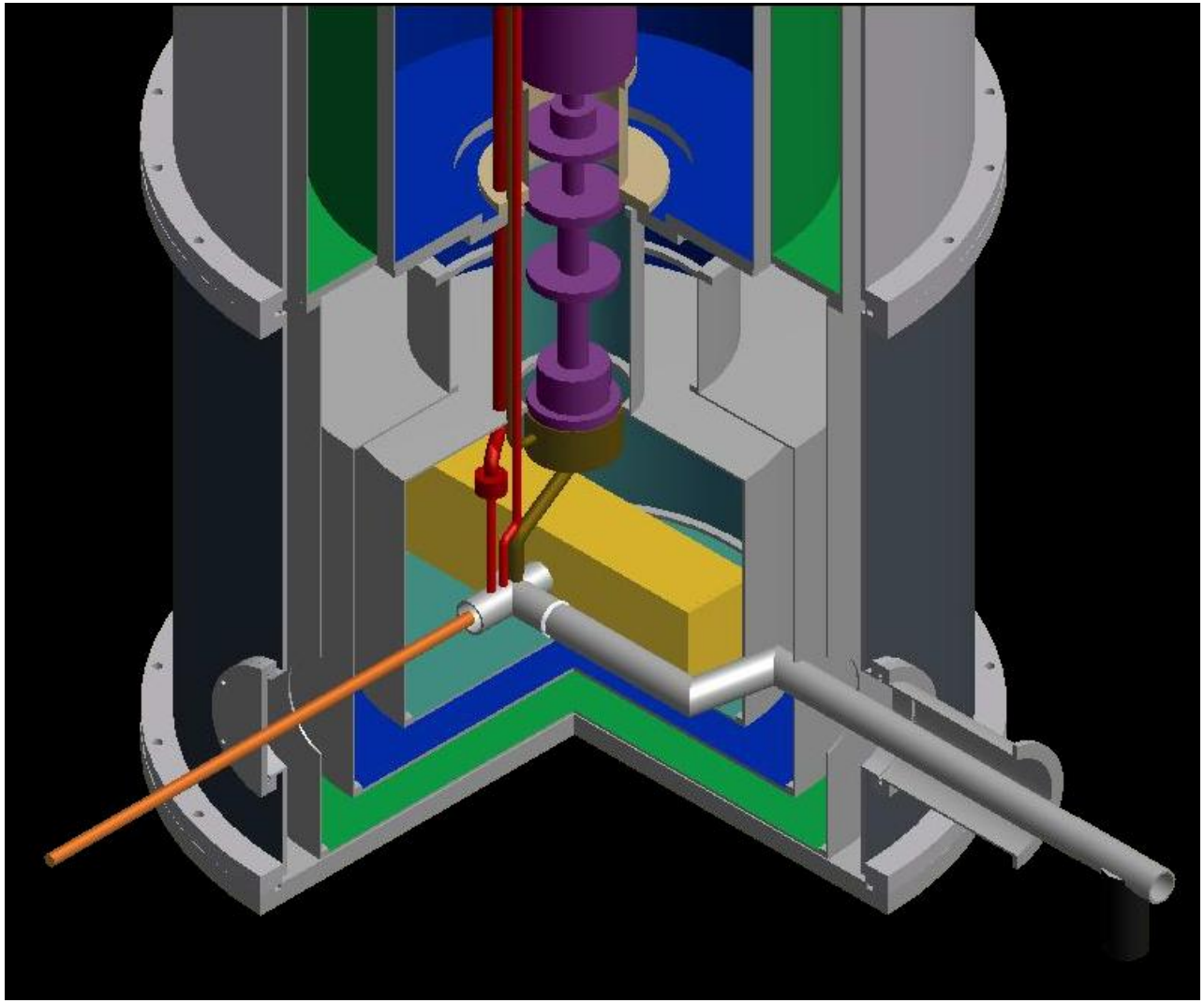

Pulstar EDM Test Setup

Schematic Layout

Revision 8

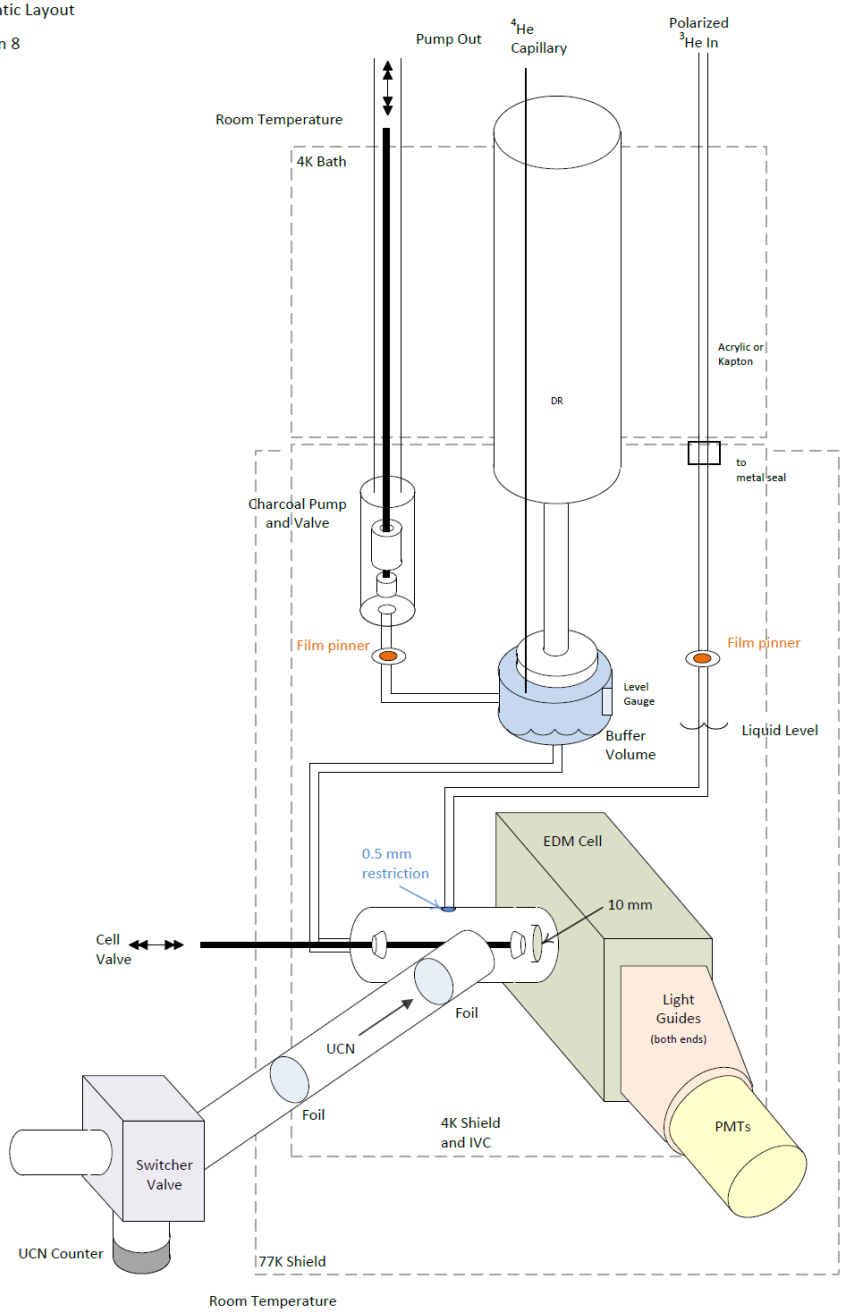

PULSTAR Systematics

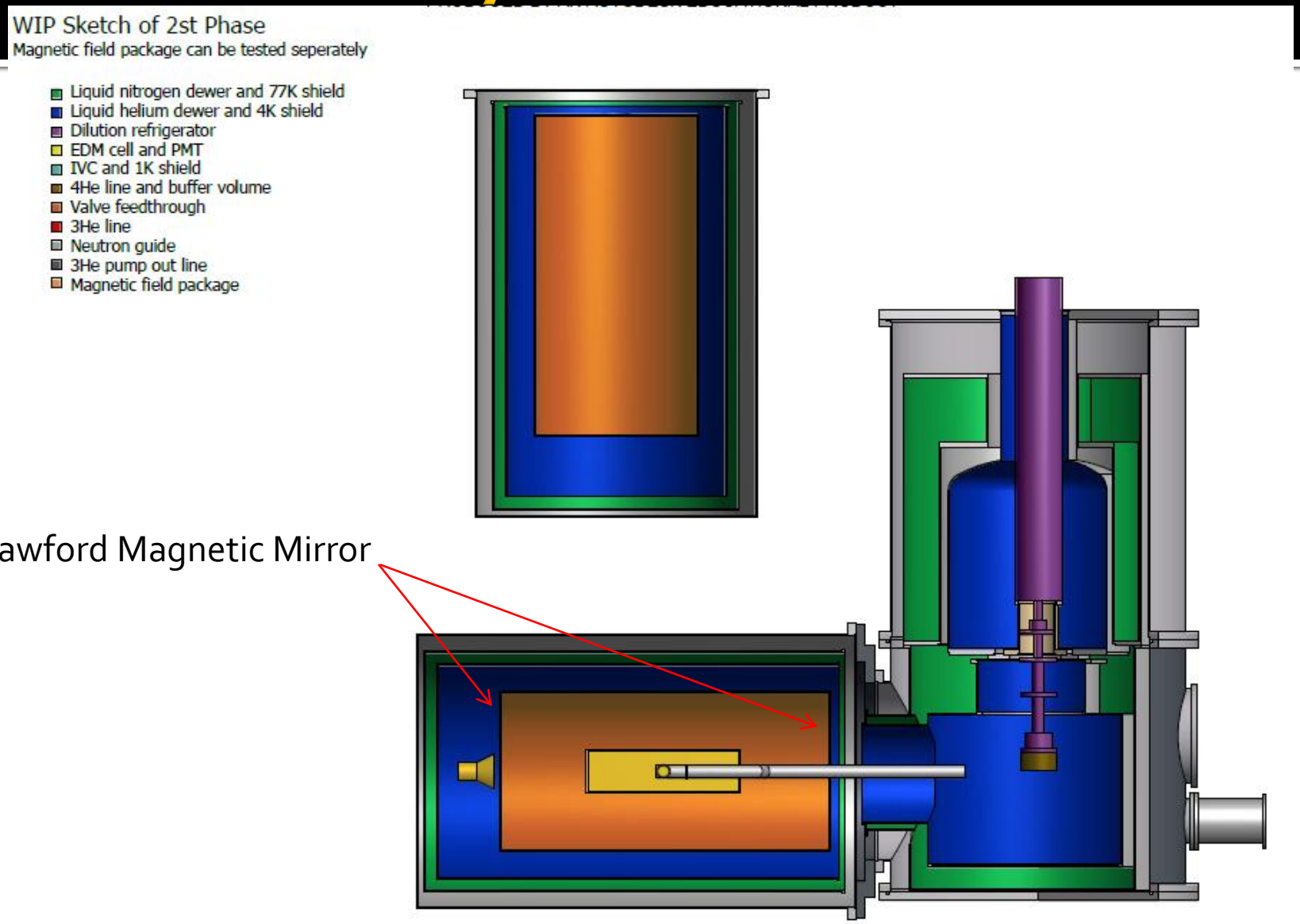

C. Crawford Magnetic Mirror

Conclusion

- Geometric phase from magnetic gradients
  - Gradients natural to coil geometry
    - PULSTAR Experiment
  - Magnetic impurities in cell walls, cell coatings, magnetic dust on coatings.
    - Cs NMOR cells prior to fabrication

False EDM for a 1 pA leakage current and a magnetic field gradient of 1.5×10^{-5}/cm

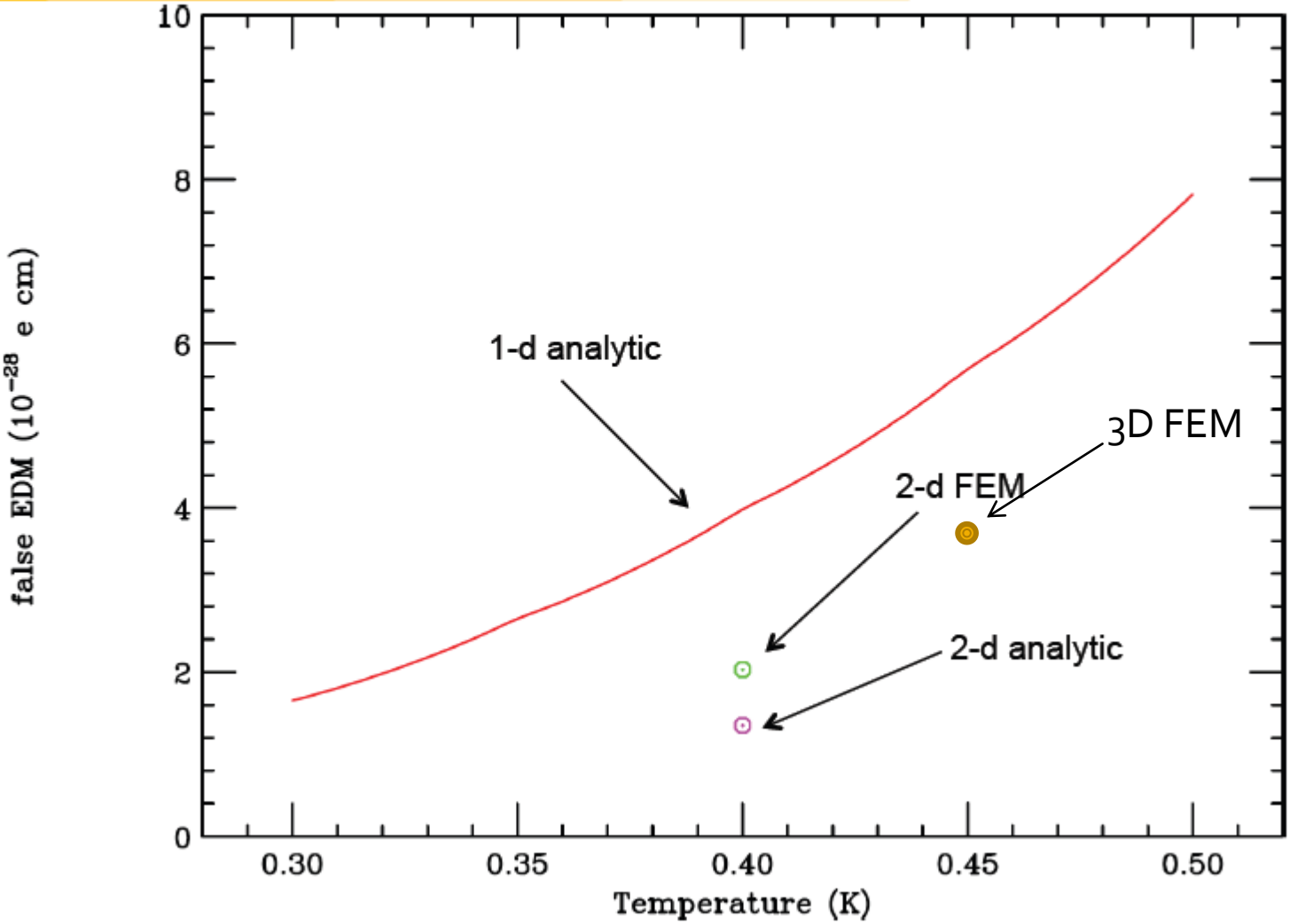

D(0.4)=977 cm²/s D(0.45)=428 cm²/s